JOURNAL OF PROPULSION AND POWER
Vol. 22, No. 3, May–June 2006

Effect of Tab Parameters on Near-Field Jet Plume Development

Parviz Behrouzi* and James J. McGuirk†
Loughborough University, Loughborough, Leicestershire LE11 3TU, United Kingdom

A full understanding of jet mixing behavior is essential in the aircraft design process, particularly when propulsion system integration issues are considered (for example, jet afterbody interactions, jet plume characterization, and jet noise reduction). The present work is motivated by an interest in unconventional jet exhaust nozzle design, specifically tabbed nozzles. The near-field mixing performance arising from a simple axisymetric jet shear layer and three-dimensional perturbed jet shear layers created via a range of solid tab designs introduced at the nozzle exit plane has been studied under subsonic and supersonic operating conditions. The effects of velocity ratio, tab shape, tab number, and tab orientation angle are investigated. Flow visualization of the tab effects is accomplished via laser-induced fluorescence in low-speed flow and schlieren imaging under supersonic conditions. The mean and rms axial velocity as well as pitot pressure and total temperature profiles have been measured along the jet centerline and on orthogonal cruciform radial traverse lines downstream of the nozzle exit. The performance of the solid tab in causing bifurcation of the jet was found to follow the same trend under both subsonic and supersonic conditions, indicating that the dominant features of the streamwise vorticity introduced by the tabs are essentially independent of the Mach number. The experimental results revealed that the decay of the jet core velocity was only weakly dependent on velocity ratio (over the range studied here), tab orientation angle, and tab shape. The mixing of the jet was, however, a strong function of the tab projected area, tab width, and tab number. The optimum tab number was found to be 2.

Nomenclature

D_n	=	nozzle exit diameter
P_c	=	corrected pitot pressure (abs. bar) at probe measuring point
P_{ISA}	=	international standard atmosphere sea-level static pressure (abs. bar)
$P_{\text{non-dim.}}$	=	non-dimensional pitot pressure
R	=	velocity ratio: nozzle exit mean axial velocity/co-flow mean axial velocity
r	=	radial direction
$T_{\text{amb.}}$	=	ambient static temperature, K
T_c	=	corrected total temperature (K) at probe measuring point
$T_{\text{non-dim.}}$	=	non-dimensional total temperature
$T_{\text{n.set}}$	=	nozzle total temperature set point (K) for a given test condition ($= NTR \times T_{\text{amb.}}$)
U	=	mean axial velocity, m/s
U_c	=	co-flow mean axial velocity, m/s
U_n	=	nozzle exit mean axial velocity, m/s
u-rms	=	rms axial velocity, m/s
u_c-rms	=	co-flow rms axial velocity, m/s
u_n-rms	=	nozzle exit rms axial velocity, m/s
x	=	axial direction
y	=	spanwise (horizontal) direction
z	=	transverse (vertical) direction

I. Introduction

EXTENSIVE research on jet mixing enhancement has been carried out over the last 50 years. Many techniques such as the use of solid tabs, acoustic excitation, and serrated nozzles have been employed and the studies up to 2001 have been usefully summarized by Seiner et al.[1] A solid tab is a small protrusion placed at the jet nozzle exit as shown in Fig. 1; each tab produces a counter-rotating streamwise vortex pair with a sense of rotation such that, between the two vortices, ambient fluid is ingested into the core of the jet. Clearly, if beneficial, one or several tabs can be attached at nozzle exit to enhance the mixing process (e.g., to effect plume signature reduction), although this may also increase the associated drag (thrust loss) penalty. Tabs appear to be a practical method for jet plume mixing enhancement in the near field, that is, between two and 10 diameters from the jet exit. Tabs have also been shown to eliminate or reduce screech noise substantially, and mixing and shock-associated noise at low frequencies, but to increase the contribution to broadband jet noise of higher frequencies. Tabs also alter the shock structure drastically in the case of jet nozzles operating at underexpanded nozzle pressure ratios (NPR).

Bradbury and Khadem[2] are usually credited with the first demonstration of the phenomenon and correctly surmised that the modification to the jet near-field development would reduce the generation of broadband jet noise. Tabs have been shown by Bohl and Foss[3] to enhance the local convective transport and mixing of ambient and jet-core fluid. The work of Samimy et al.,[4] Zaman et al.,[5] and Reeder and Samimy[6] has provided much detailed data on the effects of tabs on jet flow. Two sources for the generation of streamwise vorticity behind the tab have been identified. The dominant source comes from the pressure "hill" formed upstream of the tab (Bohl and Foss[3]). The flow deceleration upstream of the tab creates a pressure increase that, together with the strain rate associated with the boundary layer on the nozzle wall, produces a pair of counter-rotating vortices. The second source (again linked to the pressure gradients on the tab surface) is the vortex shed on flow separation from the sides of the tab. The vortex is formed as the flow goes past the tab edge. As it convects downstream, it is reoriented by the velocity gradients in the shear layer to become a streamwise vortex. If the approaching boundary layer upstream of the tab is thick, an additional vortex pair rotating in the sense opposite to the main pair is developed and is consistent with a horseshoe vortex system. The optimal tab shape has been observed to be triangular, with the tab attached directly to the nozzle wall at the jet exit without any gap.

Reeder and Zaman[7] have investigated the effect of the streamwise location of the tab and Behrouzi and McGuirk[8] have studied the effect of tab geometry on mixing rate. In particular, to reduce the drag (thrust loss) penalty of the tabs, Behrouzi and McGuirk[8]

Received 11 January 2005; revision received 22 July 2005; accepted for publication 17 October 2005.

*Research Associate, Department of Aeronautical and Automotive Engineering; P.Behrouzi@lboro.ac.uk.

†Professor of Aerodynamics, Department of Aeronautical and Automotive Engineering; J.J.McGuirk@lboro.ac.uk.

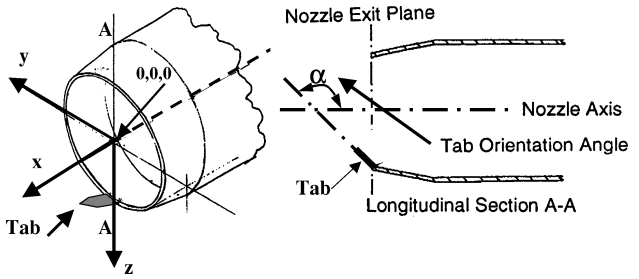

Fig. 1 Tab mounting orientation and coordinate system.

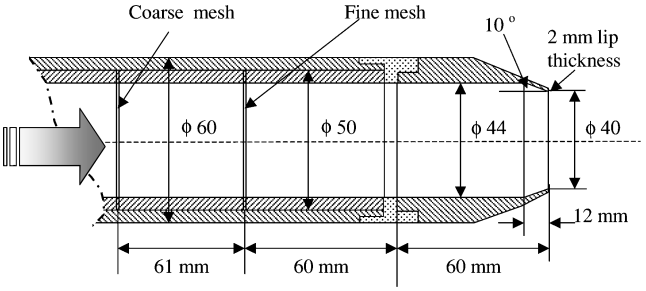

Fig. 2 Schematic design of LU40 nozzle and supply pipe.

examined various three-dimensional shapes for the tab while maintaining the same projected area. The mixing improvement for all three-dimensional shape tabs was found to be substantially reduced compared to the simple two-dimensional (i.e., thin flat plate) tab for the same projected area. All attempts to reduce the drag and performance loss penalty of the tabs were accompanied by significant reductions in tab mixing effectiveness. Bohl and Foss[9] have clearly demonstrated that the addition of secondary tabs on each side of the primary tab provides an increase in the flux of vorticity into the flow. Delta tabs (triangular tabs oriented downstream at an angle to the main flow direction) were used by Saiyed et al.[10] in a coaxial (core stream/fan stream) jet nozzle to produce strong streamwise vortices to mix the core flow aggressively with the fan flow. Some tabs protruded into the core flow and some into the fan flow. Foss and Zaman[11] have presented a detailed study of the effects of tab orientation and spacing, showing that the optimal pitch angle of a delta tab was 45 deg and the optimal spacing of an array of tabs was 1.5 tab base widths, because this configuration produced large-scale motions with peak streamwise velocity and maximized the strength of small-scale turbulent mixing. Under subsonic conditions, tabs with substantial tilt into the jet flow increase noise at all frequencies (Ahuja[12]). This is attributed to increased turbulence levels in the jet plume shear layer. Under supersonic conditions, tabs can completely eliminate the screech phenomenon. This is attributed to the thickening of the mixing layer, which inhibits the growth of instability waves, a crucial component of the feedback loop responsible for generating screech.

The flowfield of a transverse jet that is injected through a hole into a cross-flowing boundary layer has been described by Suzuki et al.[13] as an alternative mechanism for introducing streamwise vorticity. A similar concept was studied by Behrouzi and McGuirk[14] in both water flow and high-speed air jets and this concept was found to be very effective in increasing mixing (it was referred to by Behrouzi and McGuirk[14] as a "fluid tab"). The effectiveness of the fluid tab was reported to depend not only on tab flow rate, but also on tab flow exit area. It was concluded that the effectiveness of a fluid-tabbed nozzle could be optimized to the same level as that of a solid-tabbed nozzle at a fluid tab flow rate of less than 1% of the jet flow.

Experimental facilities at Loughborough University for the study of the near field of nozzle flows under static test conditions have been under development and in use to produce datasets since 1994. The present work is part of this research and is in particular concerned with the effect of various tab parameters on the enhancement of jet mixing under both subsonic and supersonic conditions.

II. Experimental Setup and Instrumentation

A. Water Tunnel Facility

The first part of this study was carried out in a specially designed and constructed water tunnel facility (WTF), which has previously been described in detail by Behrouzi and McGuirk.[8] The advantage that water facilities offer over conventional wind tunnels is that, provided only low-speed incompressible conditions are of interest, they are extremely convenient for flow visualization. In addition, because of the lower kinematic viscosity of water (by a factor of around fifteen), it is possible to reproduce a low-speed air flow in a water tunnel facility with a much lower velocity for the same Reynolds number. Due to this lower velocity, the flow time scales become proportionally large, thus leading to clearer observations of dynamic phenomena.

The rig is of recirculating design. The test section dimensions are 1.125 m long, 0.37 m wide, and 0.3 m high. The test section is made of Perspex to allow ample optical access for both laser Doppler anemometry (LDA) measurements and flow visualization. The jet nozzle unit is positioned centrally inside the test section. The water circuit consists of both a jet flow and a tunnel flow (coflow), both discharging in the same direction. Pumps extract water from a main supply tank and pump it to a large settling chamber (for the coflow) or to an overhead jet supply tank, which feeds the jet nozzle unit assembly. The jet mass flow rate is monitored via a rotameter, whereas the coflow mass-flow rate is measured using a calibrated orifice plate. Turbulence management units are provided in both coflow and jet nozzle circuits, to provide controlled and well-defined conditions at all inlets to the test section.

For experiments performed in the water tunnel, a convergent nozzle (LU40) was employed. Figure 2 presents the dimensions of this nozzle, also showing the turbulence management system. The nozzle exit diameter, nozzle boattail angle, and nozzle internal convergence angle are 40 mm, 12.5 deg, and 10 deg, respectively.

Laser Doppler anemometry is the most suitable choice of instrumentation technique for measurement of both mean and fluctuating velocity in complex turbulent three-dimensional flows. For the present study the mean velocity and turbulence fields were measured using a single-channel forward-scatter fringe-mode anemometer powered by a helium–neon laser operating at a nominal power setting of 10 mW. A further advantage of using water as a working fluid was that a plentiful supply of naturally occurring dust particles in the water formed the scattering centers so that no artificial seeding was necessary and strong signals at high data rates (of order 10 kHz) were obtained even with the low laser power used. Sensitivity to the flow direction was provided by a DANTEC 55X29 Bragg cell with variable frequency shifting made possible by a DANTEC 44N101 frequency shifter. A 310-mm focal length transmission lens was used with a beam spacing of 60 mm. The resulting signals were processed using a TSI IFA-550 processor connected to a personal computer and controlled by a ZECH-LDA Model 1400A data acquisition interface.

Laser-induced fluorescence (LIF) was used for flow visualization in the water flow experiments. Briefly, the beam from a continuous-wave argon-ion laser was converted to a 1-mm-thick sheet of light by a cylindrical lens. The sheet was directed into the flow regions of interest. Fluorescent dye was added to the jet flow, and the laser illumination caused the dye tracer to fluorescence. The emitted light was imaged via a still camera. The selection of fluorescent dye was made according to considerations such as solubility in water and absorption and emission spectra in the range of wavelengths appropriate for existing instrumentation, as well as toxicity factors. Rhodamine B was used as the fluorescent dye. Note that, although mixing enhancement is the prime interest here, no attempt has been made to evaluate the increase in mass flow within the jet with downstream distance, because this would require measurement and integration over the entire jet cross-section, which is expensive and time-consuming. This was done by Behrouzi and McGuirk,[8] who showed that even for a bifurcated jet, there is a good correlation between mass-flow increase due to jet/ambient mixing and the decrease of the peak

velocity due to momentum diffusion. Hence, in this paper, changes in the rate of the velocity decay are used to estimate comparative trends in mixing rates.

B. High-Pressure Nozzle Test Facility

The second part of the study was carried out in a specially designed and constructed high-pressure and heated air-flow rig for nozzle flow studies. The Loughborough University High-Pressure Nozzle Test Facility (HPNTF) consists of a compressor, storage tanks, delivery pipelines to the test cell, control valves, combustion unit, rig control panel, and rig instrumentation. The compressor draws 0.86 m^3/s of ambient air (approx. 1 kg/s) at the inlet and supplies high-pressure air with a maximum downstream pressure of 200 psig. The eight air storage tanks have a volume of 110 m^3 and act as a buffer to damp pressure fluctuations as well as providing an air supply for the HPNTF to be run in blowdown mode. A desiccant-type compressed air drier is used for drying the high-pressure air to a dewpoint of -40°C. A computer-controlled valve is employed to hold the mass flow rate constant through the nozzle. The facility can be used in continuous or blowdown mode. In blowdown mode the tanks are first filled to a substantially higher pressure than the desired NPR for the selected test operating point. The automatic control valve allows the rig to run with decreasing pressure upstream of the valve but fixed nozzle pressure until the supply system pressure approaches too close to the operating set point. Typical blowdown run times are between 15 s and 30 min depending on the NPR. To accomplish heating of the air supplied to the jet nozzle, a combustor is employed. The combustion unit used is part of an ex-test rig for single-can combustors for the Rolls-Royce Spey, and later Tay, series of engines. Figure 3 presents a view of a jet nozzle with tabs installed fitted to the HPNTF.

For experiments performed in the HPNTF, a convergent nozzle (LU60) was selected and tested with both hot and cold jets under subsonic and supersonic (screech-free) jet exit conditions. Figure 4 presents the dimensions of this nozzle. The nozzle exit diameter, nozzle boattail angle, and nozzle internal convergence angle are 60 mm, 12.4 deg, and 11 deg, respectively. The nozzle lip thickness was increased to 7 mm to allow secure installation of the tabs. Total temperature and pitot pressure measurements were performed in all HPNTF tests using a specially made combined temperature/pressure probe. The probe was fabricated from stainless steel hypodermic tubes of 2.5-mm diameter, accommodating a vented unshielded thermocouple bead of 1-mm diameter and a 1.1-mm hypodermic Pitot probe.

For HPNTF experiments, the schlieren technique was a convenient method of establishing the position and shape of shock waves. The schlieren method depends on the deflection of a ray of parallel light from its undisturbed path when it passes through a fluid medium in which there is a gradient of the refractive index normal to the ray. The schlieren system used for the test cases performed here was of a Z-type design and consisted of a mercury vapor lamp, two concave mirrors of 10-in. diameter, two plane mirrors of 12-in. diameter, and a knife-edge unit. Schlieren pictures were taken of the jet plume just downstream of the nozzle exit.

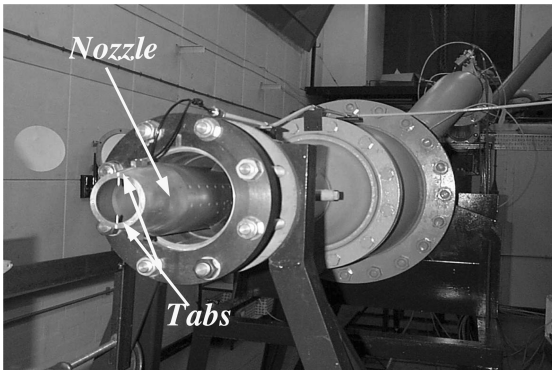

Fig. 3 Nozzle unit mounted in the HPNTF.

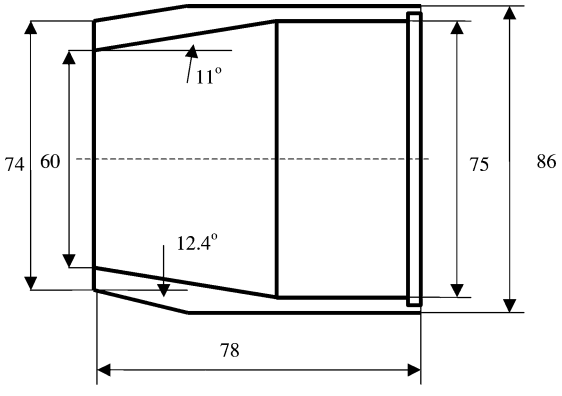

Fig. 4 Schematic design of LU60 nozzle.

C. Tab Design

Figure 1 shows details of the tab installation. Tabs were small pieces of metal (of different shapes; see later) and were attached at the nozzle exit plane. The tab was mounted so that the normal to the tab surface and the nozzle axis were in the same plane. Where more than one tab was used, tabs were positioned equispaced around the nozzle circumference. Eight different tab shapes were employed in the present study, whose dimensions are shown in Fig. 5. The description of each tab type is presented in Table 1.

Tab types 1 to 4 were manufactured from 0.2 mm brass sheet and were silver-soldered into slots machined at the appropriate location in the nozzle lip.[15] Tab types 5 to 8 were fabricated from 1 mm stainless steel sheet and were screwed to the lip of the nozzle as shown in Fig. 6. Tabs were positioned at different locations and at

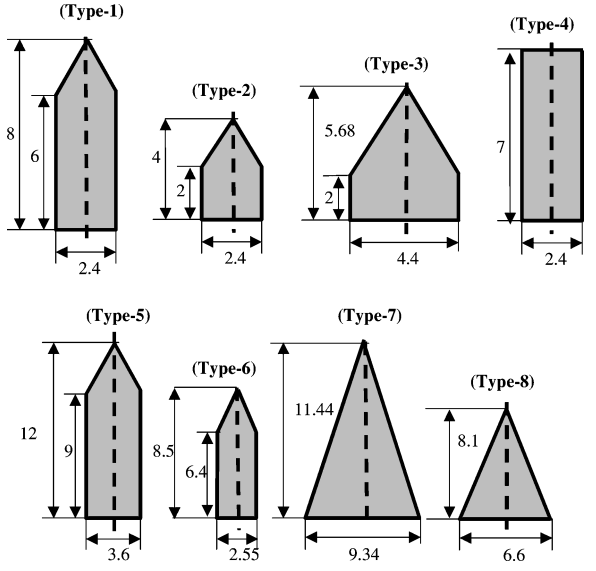

Fig. 5 Dimensions (mm) of tabs used in the WTF (top row) and HPNTF (bottom row).

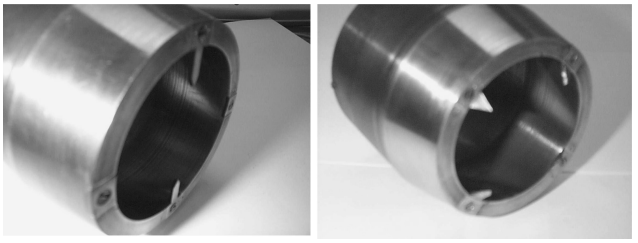

Fig. 6 Photos of the LU60 nozzle with twin tabs (type 5) and four tabs (type 8).

Table 1 Description of tab types

Tab type	Description	Area mm^2	Projected blockage area%	Nozzle	Test rig
1	Baseline-1 tab shape as reported by Ahuja and Brown[15]	16.80	0.669	LU40	WTF
2	Half Baseline-1 height	7.20	0.287	LU40	WTF
3	Wider but the same area as Baseline-1	16.90	0.669	LU40	WTF
4	Flat topped, same area as Baseline-1	16.80	0.669	LU40	WTF
5	Baseline-2(as Baseline-1 but scaled for LU60 nozzle)	37.80	0.669	LU60	HPNTF
6	Half Baseline-2 area	19.00	0.336	LU60	HPNTF
7	Delta shape, same area as Baseline-2, as used by Reeder and Samimy[6]	37.79	0.669	LU60	HPNTF
8	Delta shape, half Baseline-2 area	18.91	0.335	LU60	HPNTF

Table 2 Nozzle exit flow conditions for water tunnel tests

Test case	Nozzle exit velocity mean, m/s	Nozzle exit velocity rms, m/s	Jet Reynolds number	R (Jet to coflow velocity ratio)
1	0.53	0.018	20,400	3
2	0.44	0.015	17,000	2.5
3	0.36	0.014	13,600	2
4	0.27	0.012	10,200	1.5

different orientation angles. The number of tabs was varied from 1 to 4. Figure 6 presents photos of the LU60 nozzle mounted with twin tabs (type 5; left photo) and four tabs (type-8; right photo). The Delta tabs (types 7 and 8) were mounted inclined with their apex pointing 45 deg downstream (a tab orientation angle of 135 deg).

III. Experimental Procedure

In the coordinate system used below to report measurements, the origin is located at the nozzle center in its exit plane (Figure 1; left); the longitudinal (x) coordinate is oriented along the jet axis (positive downstream), the (z) coordinate is positive vertically downward, and the spanwise (y) coordinate has its positive direction such that a right-handed orthogonal set is formed.

A. Water Tunnel Facility

The uniformity of the mean and rms turbulence intensity velocities at nozzle exit and in the coflow plane surrounding the nozzle unit were measured. For the conditions under which measurements were carried out, the mean velocity was uniform over the central 85% of the jet diameter. The uniformity of the coflow mean velocity was also checked and also found to be flat over the central 80% of the tunnel cross section. The boundary layer thickness of the flow on the jet nozzle outside wall was measured as 0.25 D_n at nozzle exit and was uniform around the nozzle circumference.

For all tests the coflow velocity and associated rms level were held constant at 0.17 m/s (tunnel Reynolds number 28,000) and 0.008 m/s (turbulence intensity 5%), respectively. The nozzle exit velocity was then fixed at four different levels, as shown in Table 2.

Before each test, the water tunnel was run under the specified test condition for at least 1 h. The jet and coflow velocities were checked using the LDA system before commencement of measurements.

No corrections have been made for sampling bias in the LDA results. Any associated errors were minimized using high data rates compared to typical velocity fluctuation rates. The signal processor was operated in trigger mode such that data were acquired at fixed time intervals; a typical data rate used was 2 kHz. To minimize statistical (random) errors, the number of instantaneous velocity values used to form time averages was set at the large value of 40,000 (sampling time 20 s) for all data points.

The effect of the jet/coflow velocity ratio (R) was studied using the plain LU40 nozzle. Three tests were then performed with tab type-1 at orientation angles of 30, 90, and 150 deg at a fixed velocity ratio of 3. The effect of tab type on jet mixing enhancement at a fixed velocity ratio of 3 was studied using all four sets of tabs, types 1 to 4. Finally, the effect of the number of tabs (1 to 4) on the decay of the jet core velocity and the spreading of the jet was studied using tab type 1 at a velocity ratio of 3.

B. High-Pressure Nozzle Test Facility

The effect of the type and number of tabs on jet plume development was investigated under supersonic flow conditions in the HPNTF. The LU60 nozzle was tested under mildly underexpanded conditions (NPR = 2). Five tab configurations were investigated, namely the plain LU60 nozzle, the LU60 nozzle with two Baseline-2 tabs (type-5), with two delta tabs (type-7), with four normal tabs (type-6), and with four delta tabs (type-8). It in important to note that the projected area of each tab in the two-tab experiments was twice that in the four-tab experiments; in other words, the total blockage area for all four cases was the same. Tests were carried out for all five tab configurations under both cold ($T_{\text{n.set}} = 300$ K, jet Reynolds number = 348,300) and hot ($T_{\text{n.set}} = 600$ K, jet Reynolds number = 147,500) conditions. Schlieren images were taken for the majority of these cases. Pitot pressure and total temperature profiles (for hot runs) were measured along the jet center line and along transverse cruciform lines at $x/D_n = 0.25$, 5, and 10 downstream of the nozzle exit.

Pitot pressure measurements were corrected for the effects of small nozzle supply pressure fluctuations during a run, for any difference between ambient pressure during any particular run and a reference standard atmospheric pressure ($P_{\text{ISA}} = 1.0135 \times 10^5$ Pa), and finally for differences between the desired nozzle pressure set point and the average nozzle supply pressure during a given run (around 1% drift was possible during a blowdown run). The final corrected and nondimensionalized Pitot pressure was calculated as follows:

$$P_{\text{non-dim.}} = P_c / P_{\text{ISA}}$$

A similar correction and nondimensionalization procedure was used for total temperature measurements. The raw measured total temperatures were corrected for the effects of nozzle supply temperature fluctuations during a run, and for any difference between desired nozzle temperature set point and the average nozzle supply temperature during a run. The final corrected and nondimensionalized total temperature was calculated as follows:

$$T_{\text{non-dim.}} = (T_c - T_{\text{amb.}})/(T_{\text{n,set}} - T_{\text{amb.}})$$

The stability/repeatability of the measurements was also established. The maximum nozzle pressure and temperature deviations from a test set value for a typical run (hot or cold) were measured and are summarized in Table 3.

IV. Results and Discussion

A. Flow Visualization

Figures 7a and 7b present a sample of water-tunnel LIF visualization photos of the jet cross section at $x/D_n = 2$ with and without 2 Baseline-1 tabs located on the z-axis. Figures 7c and 7d present contour plots of axial velocity measurements at the same location

using the LDA system (Behrouzi and McGuirk[8]). Distortion created by the streamwise vorticity introduced by the tabs is very clear to see in both qualitative and quantitative datasets with bifurcation of the maximum velocity occurring on either side of the jet centerline. The effect of the tabs is to cause the jet core to split into two parts and hence increase the interfacial area of the mixing layer between the jet and coflow streams. This speeds up the mixing process and shortens the jet potential core length.

Table 3 Stability of nozzle flow condition for different flow regimes

Flow regime	Max. pressure deviation %	Max. temperature deviation %
Cold subsonic	±1.3	——
Cold supersonic	±0.5	——
Hot subsonic	±0.6	±0.35
Hot supersonic	±0.85	±1.35

Figure 8 presents schlieren images of the jet plume for the LU60 nozzle in the HPNTF fitted with or without different tab shapes and numbers under cold supersonic test conditions (NPR = 3, $T_{n.set} = 300$ K). Because the shock pattern details are more obvious at higher nozzle pressure ratio, NPR = 3 was chosen for capturing the schlieren images. The effect of the tab number and the tab type on enhancing mixing is identifiable in the schlieren images via the more rapid expansion of the mixing layers emanating from the nozzle lip, and also the tabs themselves in (for example) the bottom compared with the top picture. The delta and normal (Baseline-2) tabs created similar perturbations to the plain nozzle shock pattern, adding new oblique shocks to the basic plain nozzle diamond shock cell structure. Although the projected area of a Baseline-2 tab is the same as a delta tab, it creates a stronger/more dominant additional shock patteren (especially in the first cell).

B. Effect of Velocity Ratio

In the water tunnel experiments, a down-tunnel coflow directed parallel to the jet discharge had been incorporated because initial

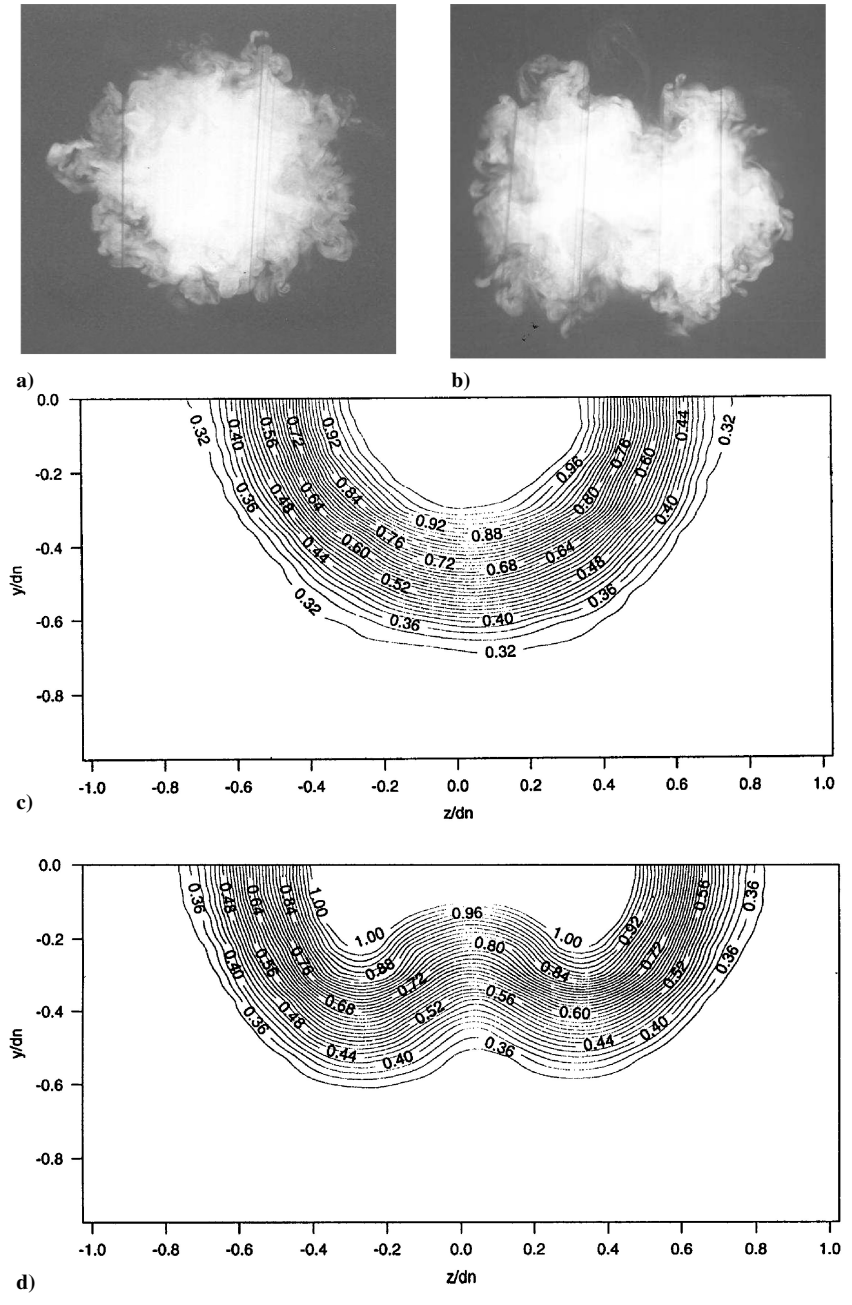

Fig. 7 LIF images of the jet cross section and measured nondimensional axial velocity contours at x/D_n = 2 for a, c) plain nozzle, b, d) twin-tabbed LU40 nozzle.

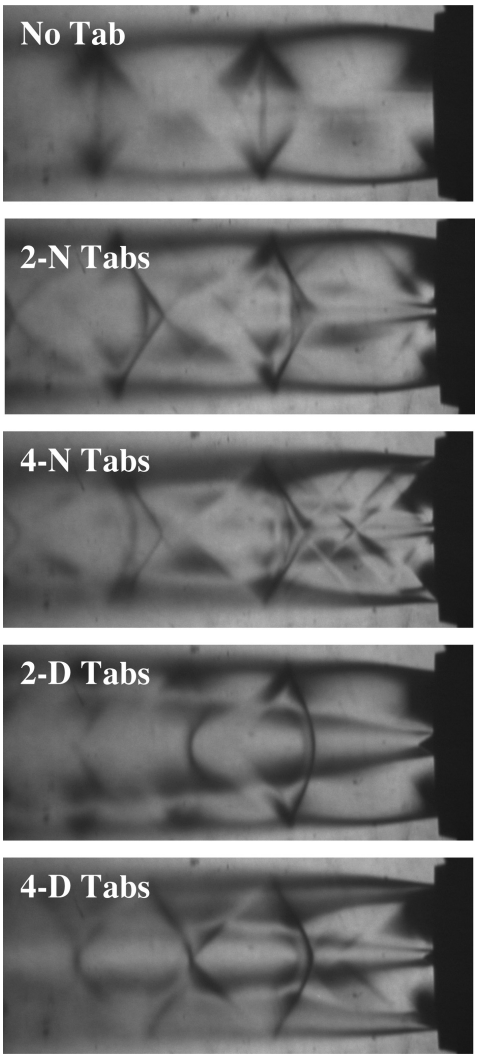

Fig. 8 Schlieren images of the jet plume showing the effect of tab number under cold supersonic flow conditions (NPR = 3).

measurements indicated that without coflow the confined and restricted size of the tunnel cross section would cause unstable jet behavior in the downstream region. A small coflow stabilized this. There was some concern, however, that the presence of the coflow would interfere with the jet shear layer development for both plain and tabbed nozzles. It was necessary to establish that this interference was negligible, at least in the near-field region of interest. It was for this reason that a series of jet/coflow velocity ratios were studied. The effect of velocity ratios 1.5, 2, 2.5, and 3 was examined. The LU40 plain nozzle (without any tab) was employed. Figures 9–12 present the results of the LDA measurements. The effect of the velocity ratio on the decay of the centerline jet mean axial velocity and rms level up to 11 jet diameters downstream is plotted in Fig. 9. As expected, and also reported by Bradbury and Khadem,[2] no noticeable direct effect of the velocity ratio on the jet centerline decay can be observed in the region measured. At the furthest distance downstream, the results are just starting to separate in the expected manner with the highest velocity ratio giving a slightly faster decay rate. The jet nozzle exit turbulence intensity is unlikely to have much influence on the decay of the core mean velocity because it has an intensity level that is small compared to that found in the mixing layer (4% compared to 20%). The turbulence level in the jet core therefore remains independent of velocity ratio up to five jet diameters downstream of the jet (Fig. 9), that is, up to the end of the jet potential core. However, after the jet edge mixing layer has penetrated to the centerline, the increase of jet turbulence intensity is strongly influenced by the velocity ratio, with higher values of R giving a more rapid rise in turbulence level.

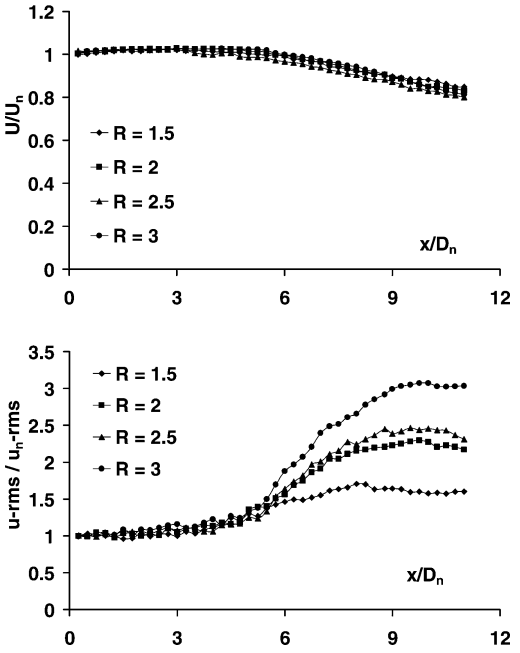

Fig. 9 Nondimensional mean (upper) and rms (lower) axial velocity along the jet centerline showing the effect of velocity ratio.

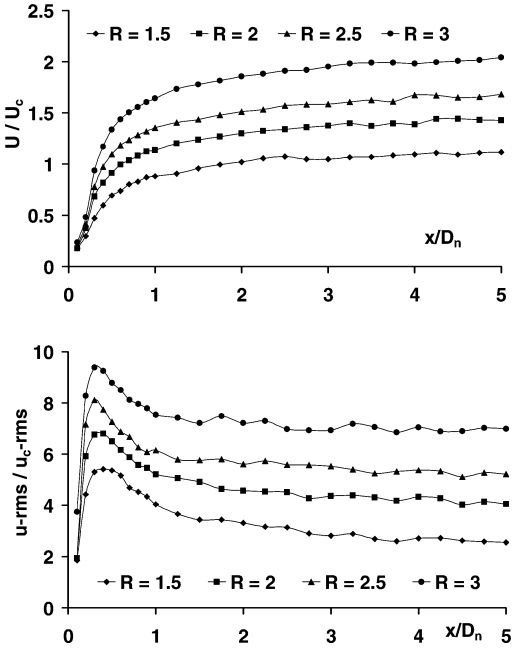

Fig. 10 Nondimensional mean (upper) and rms (lower) axial velocity along a line emanating from the nozzle lip ($r/D_n = 0.5$) showing the effect of velocity ratio.

The effect of velocity ratio on the mean and rms axial velocity along a line emanating from the nozzle lip ($r/D_n = 0.5$) is shown in Fig. 10. Both mean and rms axial velocity development inside the mixing layer are directly dependent on the velocity ratio across the layer, and at higher values of R a stronger jet mixing layer is created. This explains the sensitivity to velocity ratio noted on the centerline when the mixing layer reaches the jet axis. Figure 10 indicates, however, that the trend of mean axial velocity development is still similar at all values of R. Figures 11 and 12 show the spread of the mean and rms axial velocity profiles in the radial direction at $x/D_n = 5$ and 10. The spread of the jet is slightly larger for the higher velocity ratios as expected. A slight misalignment of the jet may be noted at the furthest downstream $x/D_n = 10$ station in the small departure from symmetry, but this does not seem to be

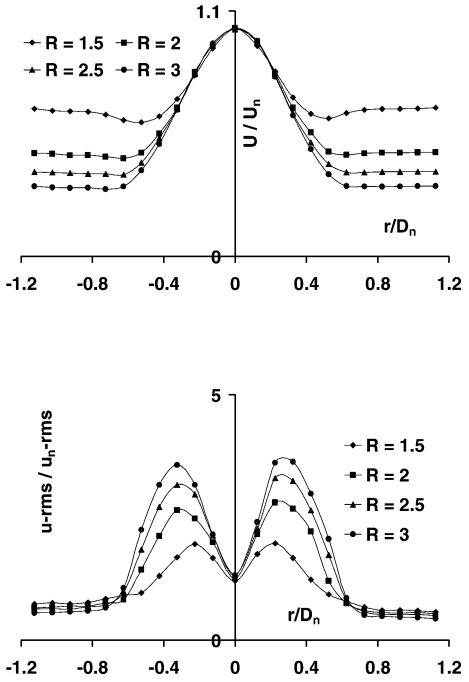

Fig. 11 Nondimensional mean (upper) and rms (lower) axial velocity in the transverse (radial) direction ($x/D_n = 5$) showing the effect of velocity ratio.

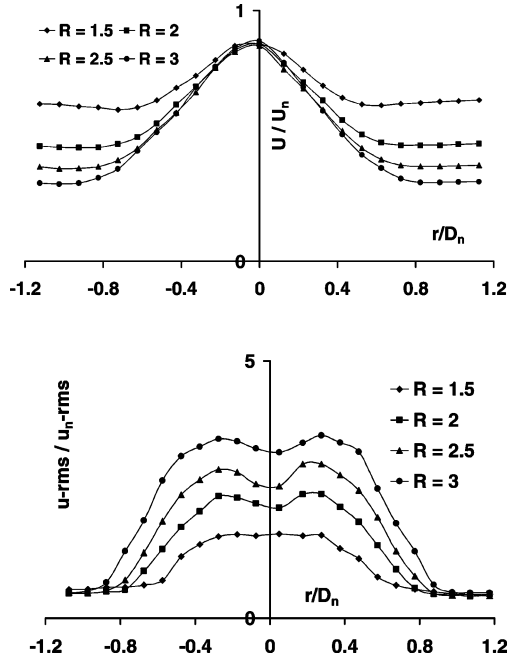

Fig. 12 Nondimensional mean (upper) and rms (lower) axial velocity in the transverse (radial) direction ($x/D_n = 10$) showing the effect of velocity ratio.

serious. At $x/D_n = 5$, the peak turbulence levels in the two mixing layers are still separate (at all values of R), whereas merging has clearly taken place by $x/D_n = 10$ (again at all R values). From these results it was determined that, although the velocity ratio clearly affects absolute levels of, for example, turbulence in the near-field region of interest ($x/D_n < 10$), the development trends were not strongly dependent on R. A velocity ratio study was also carried out in the twin tab case, but similar observations were made. It was decided, therefore, to concentrate further measurements on the $R = 3$ case because this corresponded to the weakest coflow (and hence approximated closest to stagnant ambient conditions), but the downstream jet behavior was still well stabilized at this value of R.

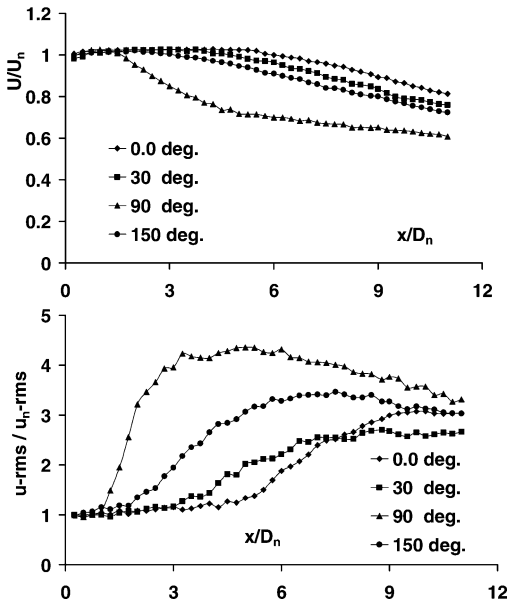

Fig. 13 Nondimensional mean (upper) and rms (lower) axial velocity along the jet centerline showing the effect of tab angle.

C. Effect of Tab Orientation Angle

The effect of varying the orientation angle of a single Baseline-1 tab was studied next. Angles of 30, 90, and 150 deg were tested in the water tunnel. Measurements of the jet flowfield were performed and a selection of results are compared with the no-tab data and presented in Fig. 13. First of all, the effect of the presence of the tab in increasing the decay of the jet core velocity and accelerating the rise of the centerline turbulence intensity (hence enhanced mixing) is quite obvious. The potential core length was reduced to around $1D_n$, $2D_n$, and $4D_n$ for tab angles of 90, 150, and 30 deg, respectively. The rapid rise of core turbulence intensity is also interesting. In the plane of measurement, which contains the tab, because use of a single tab introduces an asymmetry, the jet moves off centerline (by around $0.3D_n$ over the $10D_n$ near-field distance). Although this is not an excessive level of asymmetry (the jet has almost doubled in diameter by $x/D_n = 10$), it should be noted that the tunnel centerline data presented in Fig. 13 must as a consequence overemphasize the enhanced mixing performance of a single tab. Nevertheless, a potential core length reduction from around $5D_n$ to $1D_n$ shows the strength of the effect that a tab can induce.

The similarity between the results for tab angles of 30 and 150 deg is clear, although Fig. 13 does show that a downstream inclination is superior to an upstream lean (most visible in the turbulence data). There is, however, a noticeable difference and improvement brought about by an orientation angle of 90 deg. For this experiment the tab height was constant as tab angle varied; therefore the projected area (perpendicular to the jet flow) for a tab with an orientation angle of 90 deg is 50% more than for the other two tabs and this certainly contributes to the differences mentioned above. Although the projected area does exert a dominant effect, this does not tell the whole story. Orientation angles of 30 and 150 deg have the same projected area, but the downstream angled tabs (150 deg) have a clearly greater beneficial effect on mixing. This is consistent with the observations made by Samimy et al.[4] and Zaman et al.[5] and is related to the different streamwise vortices produced by upstream and downstream angled tabs.

D. Effect of Tab Type

An examination of the effect of tab type was carried out under both subsonic (WTF) and supersonic (HPNTF) flow conditions. For the WTF tests, a twin Baseline-1 tabbed nozzle was employed to avoid the asymmetry problem mentioned previously for a single tab nozzle. Figure 14 shows the decay of mean axial velocity and the rise of rms axial velocity along the jet centerline for four tab

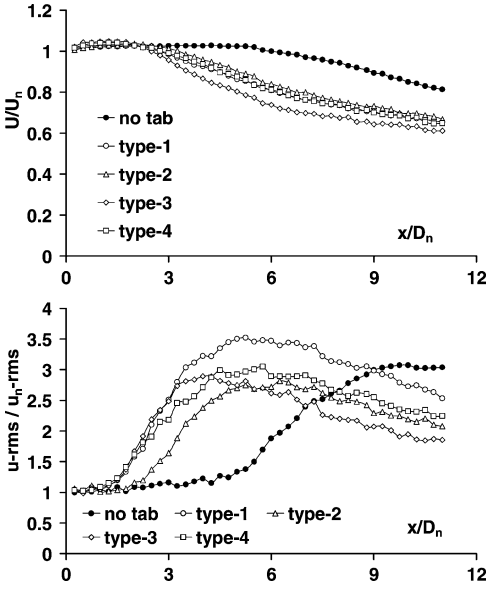

Fig. 14 Nondimensional mean (upper) and rms (lower) axial velocity along the jet centerline showing the effect of tab type.

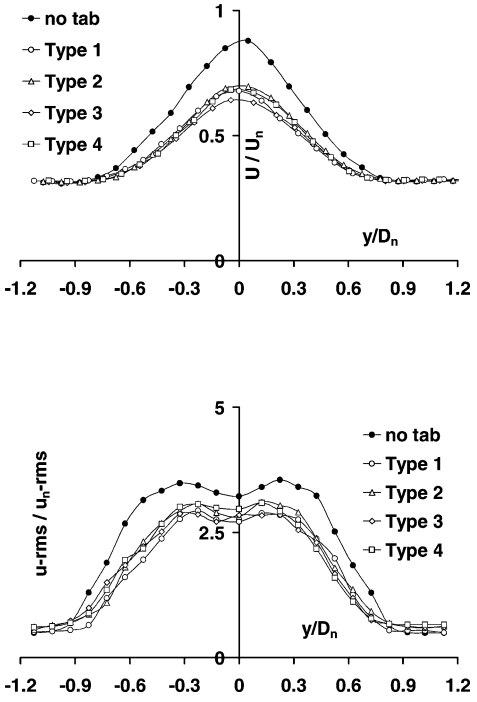

Fig. 15 Nondimensional mean (upper) and rms (lower) axial velocity in the transverse (radial) direction ($x/D_n = 10$) showing the effect of tab type.

designs (types 1 to 4). The results for tab type 1 and type 4 are quite similar; hence, for the same projected area, the precise shape of the tab (in particular at its upper end) does not seem to have a significant influence on the mixing process. The results from tab type 1 are better than those from tab type 2, but this is caused mainly by the increase in projected area. Finally, the effect of tab width (at constant projected area) can be seen by comparing the results of tab type 1 and type 3. These show a considerable effect on the decay of the jet core due to the increase in tab width. Figure 15 shows profiles of jet mean and rms axial velocities in the radial direction at $x/D_n = 10$ downstream of the jet exit. The twin tabs bifurcate the jet and the spread of the jet is clearly different in the vertical and horizontal planes. This indicates the strong three-dimensional flowfield produced by the tab and is consistent with the jet cross section shown in Fig. 7. The spread of the jet is narrower in the plane

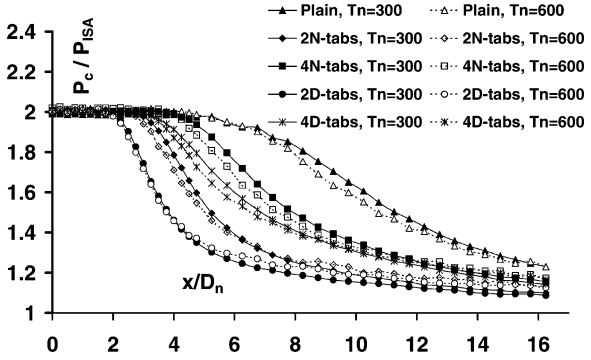

Fig. 16 Nondimensional pitot pressure along the jet centerline showing the effect of tab type, tab number, and nozzle exit temperature on jet development (LU60, NPR = 2).

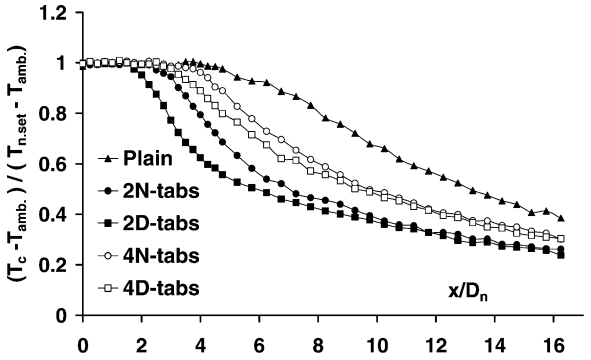

Fig. 17 Nondimensional total temperature along the jet centerline showing the effect of tab type and tab number on jet development at nozzle exit temperature for (LU60, NPR = 2, $T_{n.set}$ = 600 K).

containing the tabs, and wider in the orthogonal plane. This feature was also observed in the results of Bradbury and Khadem[2] and in the flow visualization results of Samimy et al.[4] and Zaman et al.[5]

All these data were extracted from WTF testing and hence excluded compressibility effects. To ensure that any conclusions drawn are not restricted to incompressible flows, the second part of this study was performed for high-speed flow, with the effect of tab type on jet development being emphasized. The LU60 nozzle was employed. Five test configurations were investigated, namely the plain LU60 nozzle, the same nozzle with two Baseline-2 tabs (type 5), with two delta tabs (type 7), with four normal tabs (type 6), and finally with four delta tabs (type 8). It is important to note that the total blockage area of *all* tabbed nozzles used in these tests was the same. Tests were performed under two nozzle flow conditions, namely cold supersonic (NPR = 2, $T_{n.set} = 300$ K, $Re = 348{,}300$) and hot supersonic (NPR = 2, $T_{n.set} = 600$ K, $Re = 147{,}500$). The variation of the nondimensional pitot pressure and total temperature along the jet centerline is presented in Figs. 16 and 17 for all cases. The variation of nondimensional pitot pressure in both y and z directions at the $x/D_n = 5$ location is presented in Fig. 18.

The measured potential core lengths were $5.0D_n$, $3.0D_n$, $3.75D_n$, $1.75D_n$, and $3.0D_n$ respectively for the plain nozzle, two normal tabs, four normal tabs, two delta tabs, and four delta tabs for the supersonic cold nozzle condition. The potential core lengths for the five nozzle configurations for the supersonic hot condition were $4.5D_n$, $2.75D_n$, $3.75D_n$, $1.75D_n$, and $3.0D_n$ respectively. The plain nozzle results show, as expected, the longest potential core length; heating the jet produces a slightly shorter potential core and faster decay rate in the near field. This effect of jet temperature is just about observable in other tests with mixing enhancement tabs, although the reduction is small. For the two-delta-tabs case, which produces the shortest potential core and the fastest centerline decay rate, it seems that the mixing enhancement effect of the two delta tabs is so strong that it dominates the small temperature effect. Other conclusions that may be drawn from the data in Fig. 16 are that delta tabs are more

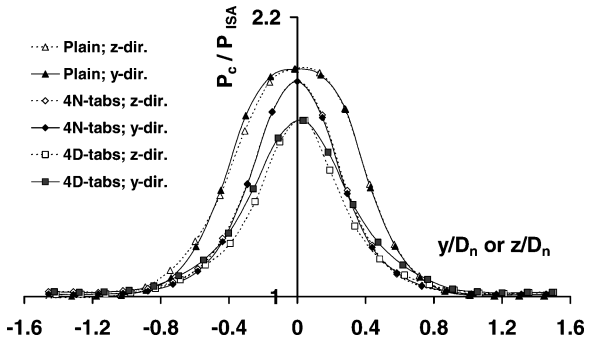

Fig. 18 Nondimensional pitot pressure in radial direction at $x/D_n = 5$ showing the effect of tab type and number (LU60, NPR = 2, $T_{n.set} = 300$ K).

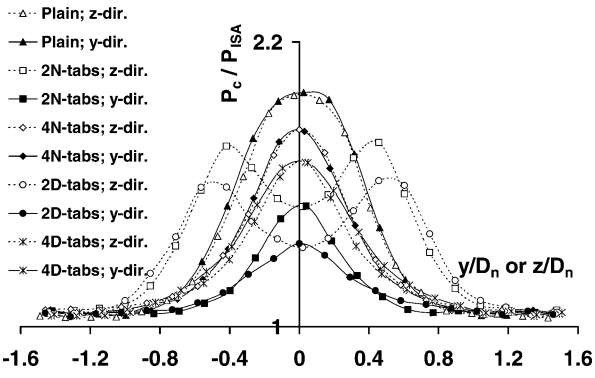

Fig. 19 Nondimensional pitot pressure in radial direction at $x/D_n = 5$ showing the effect of tab type and number (LU60, NPR = 2, $T_{n.set} = 600$ K).

effective than normal tabs (as observed by Reeder and Samimy[6]) and that 2 tabs are more effective than four. The question of why the optimum tab number is 2 is addressed further in Sec. IV.E. The order of effectiveness of the tab configurations is repeated in the total temperature data presented in Fig. 17.

The radial (both y- and z-direction) profiles for the plain nozzle in Fig. 18 show the axisymmetric nature of the flow. For mixing devices corresponding to four normal tabs, the y and z profiles fall on top of each other, but this is clearly no longer due to axisymmetry, but rather to quadrant symmetry. This is evident in that both measured y and z profiles fall *below* the plain nozzle case. The jet has therefore contracted along both y and z directions due to the inflow associated with the streamwise vortices created by the tabs. Correspondingly, the jet cross section must have increased on the 45-deg diagonal sections in between the four tabs (not shown in Fig. 18, but see cross sectional shape indicated in contours of Fig. 7). The strength of these vortices has increased for the four-delta-tab-case because the y and z profiles are now even narrower. When the tab number is reduced to 2, the tab-induced streamwise vortices are clearly further apart and can affect jet cross-sectional distortion for a larger axial distance before they begin to interfere with each other's downstream development. This is easily visible in both 2N and 2D tab results in Fig. 19 because the y and z profiles are now distinctly different (symmetry is now only across the diametric line joining the two tabs). The jet has started to bifurcate now, with the maximum jet velocity moving into the center of twin cores on either side of the tab-joining line (z-direction). This is observed for both 2N and 2D devices, but the delta tabs produce a stronger streamwise vorticity because the centerline pitot pressure has halved compared to the 2N case, the peak pressure has decreased by 20%, and the jet is clearly wider in the z direction. Although no direct measurements of entrained flow have been made, all these indications point to the interfacial mixing region between jet and ambient having been increased to optimal effect by the 2D tab devices; an estimated increase of mixing efficiency in the first $5D_n$ axial distance is at least 20%.

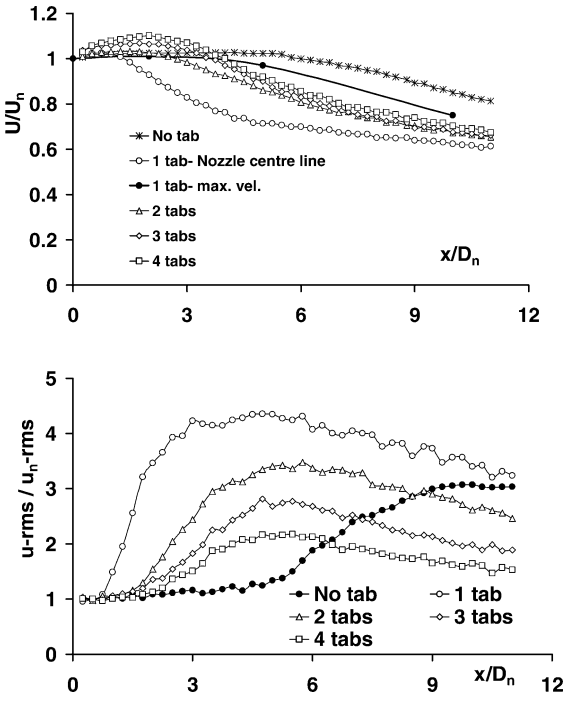

Fig. 20 Nondimensional mean (upper) and rms (lower) axial velocity along the jet centerline showing the effect of tab number.

E. Effect of Tab Number

This study was also performed at both subsonic (WTF) and supersonic conditions (HPNTF). In the WTF, the LU40 nozzle with one, two, three, and four tabs was employed. Figure 20 presents the variation of nondimensional mean and rms axial velocity along the jet centerline, showing the effect of tab number. Care must be taken when interpreting the one-tab case to allow for the effect due to asymmetry of the jet development, which will clearly also influence properties such as centerline decay as well as the jet mixing enhancement. For this reason, for the one-tab case the maximum jet velocity development deduced from radial plots is also included in Fig. 20, as well as nozzle geometric centerline measurements. It can then be seen that going beyond two tabs seems to have little additional beneficial effect on jet velocity decay rates. If anything, the three- and four-tab cases show slightly poorer performance, particularly because these will undoubtedly incur a larger pressure drop penalty. A similar conclusion may be drawn from the turbulence data shown in Fig. 20. Discounting the one-tab centerline result as anomalous for reasons explained above, the shortest potential core (point where shear layer turbulence reaches centerline) and highest turbulence level in the jet near field are again obtained with two tabs.

For the second part of this study, the effect of tab number on jet mixing enhancement was measured in the HPNTF. The effect of two and four tabs was studied as well as that of normal and delta tab types. Figures 19, 21, and 22 present variations of nondimensional pitot pressure and total temperature in the radial directions (y and z) at $x/D_n = 5$ and 10. The effect of the number of solid tabs in modifying the jet structure was made clear in the schlieren images shown in Fig. 8. The four-tab cases (normal or delta) have created more complex shock patterns than the two-tab cases. It is clear from these pictures that the flow structures created by the tabs interfere with each other much more quickly for four tabs than for two. This emphasizes again why the two-tab case is optimum; it provides maximum opportunity for the tab-induced vorticity to change the cross-sectional shape of the jet, increase the jet core/ambient interfacial area, and hence achieve extra mixing. The reduction of the measured potential core length when moving from a two-normal-tabbed nozzle to a four-tabbed nozzle was almost $1.5D_n$. This is also observed for nozzles with delta tabs. A two-tabbed nozzle induces a larger increase in jet mixing enhancement than a four-tabbed nozzle. The results presented in Figs. 19, 21, and 22 show that the effect on

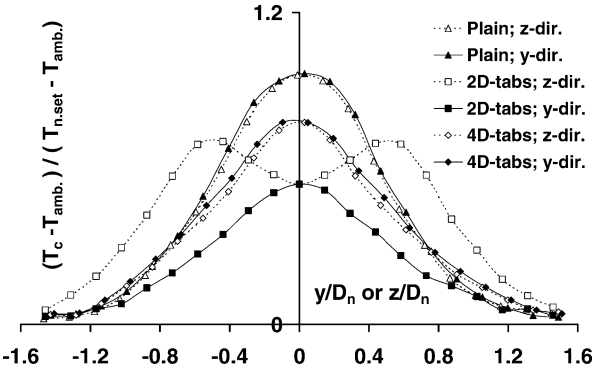

Fig. 21 Nondimensional total temperature in radial direction at x/D_n = 5 showing the effect of tab type and number (LU60, NPR = 2, $T_{n.set}$ = 600 K).

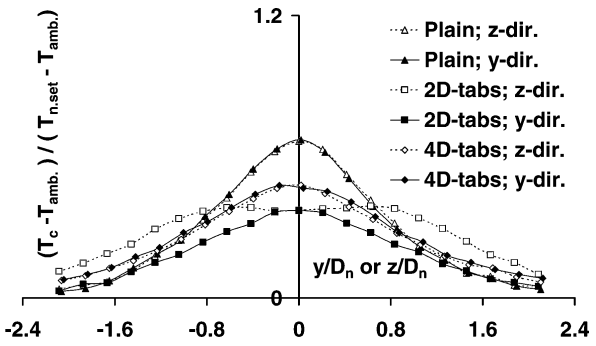

Fig. 22 Nondimensional total temperature in radial direction at x/D_n = 10 showing the effect of tab type and number (LU60, NPR = 2, $T_{n.set}$ = 600 K).

jet spreading and cross-sectional shape is essentially unaffected by jet temperature (compare Figs. 18 and 19). The peak temperature in the jet has been reduced by some 18% for 4D tabs and by about 25% for 2D tabs (Fig. 21) at $x/D_n = 5$, and about 20% (4D) and 30% (2D) at $x/D_n = 10$ (Fig. 22). These are clear indications of enhanced jet mixing.

Finally, it should be noted that for a two-normal-tabbed nozzle the performance of the various tab devices for jet mixing enhancement was found to have the same effectiveness order in both HPNTF and WTF tests. This shows that compressibility does not seen to be of prime importance in determining the effectiveness of these devices.

V. Conclusions

As part of a program of experimental work aimed at identifying and improving our understanding of nozzle flows and near-field exhaust plume mixing, specific tests have been performed to investigate the optimal shape, orientation, and location of tab vortex generators. The effect of velocity ratio, tab type, tab orientation angle, and number of tabs has been studied. Good agreement in general was achieved between tests conducted in low-speed flows (in a water tunnel) and high-speed flows (in a high-pressure air facility) on the effectiveness of a range of solid tab designs on near-field jet mixing. The trend for enhanced jet core decay rate was similar in both experimental facilities. The delta tab shape was shown to be more effective than a plain normal tab with the same projected area under both subsonic and supersonic conditions. The expected effect of hot jets in decreasing potential core length and enhancing jet decay rate was observed in the plain nozzle data, but this effect was completely dominated by the effects of the mixing devices introduced, so jet temperature was not observed to change their relative performance at all. The experimental results revealed that the decay of the jet core velocity in low-speed flows was nearly independent of velocity ratio, tab orientation angle (for the same projected area), and tab shape. However, jet mixing enhancement can be drastically affected by tab number and tab type. The mixing of the jet was found to be strongly dependant on the tab projected area, tab width, and tab number. The optimum tab number was found to be 2, because this allowed the streamwise vortices associated with the tabs to exert maximum distortion of the jet core/ambient interfacial area (and by implication jet mixing) before the various tab vortices began to interact and interfere with each other.

Acknowledgments

The authors thank K. Bradbrook and S. Nunn of BAE SYSTEMS for providing many constructive comments during the course of the work reported here. This work has been funded by BAE SYSTEMS, Warton, UK.

References

[1]Seiner, J. M., Dash, S. M., and Kenzakowski, D. C., "Historical Survey on Enhanced Mixing in Scramjet Engines," *Journal of Propulsion and Power*, Vol. 17, No. 6, 2001, pp. 1273–1286.

[2]Bradbury, L. J. S., and Khadem, A. H., "The Distortion of a Jet by Tabs," *Journal of Fluid Mechanics*, Vol. 70, Pt. 4, Aug. 1975, pp. 801–813.

[3]Bohl, D. G., and Foss, J. F., "Streamwise Vorticity and Velocity Measurements in the Near Field of a Tabbed Jet," ASME Fluids Engineering Division, Vol. 203, Turbulence in Complex Flows, Chicago, 1994.

[4]Samimy, M., Zaman, K. B. M. Q., and Reeder, M. F., "Effect of Tabs on the Flow and Noise Field of an Axisymmetric Jet," *AIAA Journal*, Vol. 31, No. 4, 1993, pp. 609–615.

[5]Zaman, K. B. M. Q., Reeder, M. F., and Samimy, M., "Control of an Axisymmetric Jet Using Vortex Generators," *Physics of Fluids A*, Vol. 6, No. 2, 1994, pp. 778–793.

[6]Reeder, M. F., and Samimy, M., "The Evolution of a Jet with Vortex-Generating Tabs: Real-Time Visualisation and Quantitative Measurements," *Journal of Fluid Mechanics*, Vol. 311, March 1996, pp. 73–118.

[7]Reeder, M. F., and Zaman, K. B. M. Q, "The Impact of Tab Location Relative to the Nozzle Exit on Jet Distortion," AIAA Paper 94-3385, 1994.

[8]Behrouzi, P., and McGuirk, J. J., "Experimental Studies of Tab Geometry Effects on Mixing Enhancement of an Axisymmetric Jet," *Japan Society of Mechanical Engineers, International Journal, Series B*, Vol. 41, No. 4, 1998, pp. 908–917.

[9]Bohl, D. G., and Foss, J. F., "Enhancement of Passive Mixing Tabs by the Addition of Secondary Tabs," AIAA Paper 96-0545, 1996.

[10]Saiyed, N. H., Mikkelsen, K. L., and Bridges, J. E., "Acoustics and Thrust of Separate-Flow Exhaust Nozzles with Mixing Devices for High-Bypass-Ratio Engines," AIAA Paper 2000-1961, 2000.

[11]Foss, J. K., and Zaman, K. B. M. Q., "Large- and Small-Scale Vertical Motion in a Shear Layer Perturbed by Tabs," *Journal of Fluid Mechanics*, Vol. 382, March 1999, pp. 307–329.

[12]Ahuja, K. K., "Mixing Enhancement and Jet Noise Reduction Through Tabs Plus Ejectors," AIAA Paper 93-4347, 1993.

[13]Suzuki, T., Nagata, M., Shizawa, T., and Honami, S., "Optimal Injection Condition of a Single Pulsed Vortex Generator Jet to Promote Cross-Stream Mixing," *Experimental Thermal and Fluid Science*, Vol. 17, No. 1–2, 1998, pp. 139–146.

[14]Behrouzi, P., and McGuirk, J. J., "Jet Mixing Enhancement Using Fluid Tabs," AIAA Paper 2004-2401, Jan. 2004.

[15]Ahuja, K. K., and Brown, W. H., "Shear Flow Control by Mechanical Tabs," AIAA Paper 89-0994, March 1989.